Loss of CYLD promotes cell invasion via ALK5 stabilization in oral squamous cell carcinoma

Satoru Shinriki[1]*, Hirofumi Jono[2, 3]*, Manabu Maeshiro[1, 4], Takuya Nakamura[4], Jianying Guo[5], Jian-Dong Li[6], Mitsuharu Ueda[5], Ryoji Yoshida[4], Masanori Shinohara[4], Hideki Nakayama[4], Hirotaka Matsui[1†], and Yukio Ando[5†]

[1]Department of Molecular Laboratory Medicine, Graduate School of Medical Sciences, Kumamoto University, Kumamoto, Japan

[2]Department of Clinical Pharmaceutical Sciences, Graduate School of Pharmaceutical Sciences, Kumamoto University, Kumamoto, Japan

[3]Department of Pharmacy, Kumamoto University Hospital, Kumamoto, Japan

[4]Department of Oral and Maxillofacial Surgery, Graduate School of Medical Sciences, Kumamoto University, Kumamoto, Japan

[5]Department of Neurology, Graduate School of Medical Sciences, Kumamoto University, Kumamoto, Japan

[6]Center for Inflammation, Immunity and Infection and Department of Biology, Georgia State University, Atlanta 30303, GA, USA

***Correspondence to:** Satoru Shinriki, Department of Molecular Laboratory Medicine,

This article has been accepted for publication and undergone full peer review but has not been through the copyediting, typesetting, pagination and proofreading process, which may lead to differences between this version and the Version of Record. Please cite this article as doi: 10.1002/path.5019

Graduate School of Medical Sciences, Kumamoto University, 1-1-1 Honjo, Chuo-ku, Kumamoto 860-8556, Japan. Phone and Fax: +81-96-373-5283; E-mail: satorus@kuh.kumamoto-u.ac.jp; Hirofumi Jono, Department of Pharmacy, Kumamoto University Hospital, 1-1-1 Honjo, Chuo-ku, Kumamoto 860-8556, Japan. Phone and Fax: +81-96-373-5823; E-mail: hjono@kuh.kumamoto-u.ac.jp.

†Contributed equally to this work and considered co-senior authors.

Running title: Association of CYLD with OSCC-related invasion

Conflict of interest: No conflicts of interest were declared.

Location of microarray data: GEO (accession number GSE100589)

Abstract

Oral squamous cell carcinoma (OSCC) has a very poor prognosis because of its highly invasive nature, and the 5-year survival rate has not changed appreciably for the past 30 years. Although cylindromatosis (CYLD), a deubiquitinating enzyme, is thought to be a potent tumour suppressor, its biological and clinical significance in OSCC is largely unknown. This study

aimed to clarify the roles of CYLD in OSCC progression. Our immunohistochemical analyses revealed significantly reduced CYLD expression in invasive areas in OSCC tissues, whereas CYLD expression was conserved in normal epithelium and carcinoma *in situ*. Furthermore, downregulation of CYLD by siRNA led to acquisition of mesenchymal features and increased migratory and invasive properties in OSCC cells and HaCaT keratinocytes. It is interesting that CYLD knockdown promoted transforming growth factor-β (TGF-β) signalling by inducing stabilization of TGF-β receptor I (ALK5) in a cell autonomous fashion. In addition, the response to exogenous TGF-β stimulation was enhanced by CYLD downregulation. The invasive phenotypes induced by CYLD knockdown were completely blocked by an ALK5 inhibitor. In addition, lower expression of CYLD was significantly associated with the clinical features of deep invasion and poor overall survival, and also with increased phosphorylation of Smad3, which is an indicator of activation of TGF-β signalling in invasive OSCC. These findings suggest that downregulation of CYLD promotes invasion with mesenchymal transition via ALK5 stabilization in OSCC cells.

Keywords: CYLD, transforming growth factor-β, ALK5, oral squamous cell carcinoma, mesenchymal transition, invasion

Introduction

Oral cancer, the sixth most frequent malignancy among all cancers, is a worldwide problem. Of the oral cancers, oral squamous cell carcinoma (OSCC) is the most common, as it accounts for more than 90% [1]. The highly invasive properties of OSCC are often associated with locoregional recurrence and lymph node metastasis in patients, and is a key factor determining the expected 5-year survival rate of approximately 50% for patients with advanced disease [2]. Thus, understanding the features and mediators of OSCC invasion is important for development of new treatment approaches. Transforming growth factor-β (TGF-β) is the best-known factor that increases tumour invasion and metastasis via induction of epithelial-to-mesenchymal transition (EMT), which is a highly coordinated cell biological mechanism that suppresses epithelial cell markers while upregulating mesenchymal ones [3-8]. Although various regulators of TGF-β signalling have been reported [9], the regulatory mechanisms are complex and depend highly on context and cell type [7,10].

The cylindromatosis gene (*CYLD*) was first identified as associated with familial cylindromatosis, a condition involving multiple skin tumours [11]. CYLD protein has a ubiquitin-specific protease (USP) domain and functions as a de-ubiquitinase, which mainly removes lysine 63 (K63)-linked polyubiquitin chains on target proteins [12,13]. Certain studies found that CYLD regulates multiple signalling pathways, including nuclear factor-κB (NF-κB), Wnt/β-catenin, c-Jun N-terminal kinase, p38 mitogen-activated protein kinase, and Hippo and Notch signalling [14-20]. CYLD also regulates microtubule dynamics by binding microtubules

via its CAP-Gly domain and indirectly the USP domain [21]. CYLD has been shown to regulate various biological processes including inflammatory and immune responses, cell cycle progression, and cancers [21]. In several types of cancer, mutation and reduced expression of CYLD were reported [22]. In addition, elimination of CYLD in mice promoted carcinogenesis in skin and liver [23,24]. However, the clinical and biological significance of CYLD in OSCC remains largely unknown.

In this study. we demonstrated that downregulation of CYLD expression promoted TGF-β signalling by stabilizing type I TGF-β receptor (ALK5) protein, thus inducing invasive phenotypes including EMT-like changes in OSCC cells.

Materials and Methods

Antibodies and reagents

Rabbit polyclonal anti-CYLD antibody for immunohistochemistry and immunoblotting were purchased from Abcam (#ab33929, Cambridge, MA, USA) and Santa Cruz Biotechnology (H-419, #sc-25779, Santa Cruz, CA, USA), respectively. Rabbit polyclonal anti-ALK5 (V-22, #sc-398) and IκB-α (C-21, #sc-371) antibodies were purchased from Santa Cruz Biotechnology. Recombinant TGF-β1 was obtained from PeproTech, Inc. (Rocky Hill, NJ, USA). ALK5 inhibitor (TGF-β RI Kinase Inhibitor II, #616452) [25] was purchased from Calbiochem (Darmstadt, Germany).

Samples from patients

Initial biopsy specimens were obtained from patients with oral carcinoma *in situ* (CIS) (n = 45) or invasive OSCC (n = 82) who subsequently underwent surgery with curative intent at the Department of Oral and Maxillofacial Surgery, Kumamoto University Hospital, between 1999 and 2004. Forty-nine men and 33 women with invasive OSCC, with an average age (± SD) of 67.8 ± 11.0 yr, were enrolled in the study. Samples of normal lower gingival mucosa were obtained from 10 healthy volunteers. Tissue samples for immunohistochemistry were fixed with 10% formalin before processing. This study has been approved by the ethical committee at Kumamoto University.

Immunohistochemistry

Formalin-fixed specimens of clinical tissues were embedded in paraffin, cut into 5-μm-thick sections, and mounted on slides. These sections were dewaxed in xylene and then rehydrated in descending concentrations of alcohol. Endogenous peroxidase was blocked via a 30-min incubation of slides with 3% hydrogen peroxide. After slides were washed with PBS for 5 min, a non-specific staining blocking reagent (DAKO, Glostrup, Denmark) was used for 10 min to block non-specific background staining, followed by overnight incubation at 4 °C with antibodies against CYLD (1:50), laminin γ2 (1:200) (D4B5, #MAB19562, Chemicon, Temecula, CA, USA), or pSmad3 (1:100) (C25A9, #9520, Cell Signaling, Tokyo, Japan) diluted in PBS containing 1% BSA. Slides were rinsed with PBS for 5 min, incubated with biotin-conjugated IgG for 1 h, and washed again with PBS, followed by incubation with HRP-conjugated streptavidin for 1 h. 3,3-Diaminobenzidine (DAKO) was used to develop chromogen. Slides were lightly counterstained with haematoxylin for 30 s before dehydration and mounting. PBS and normal isotype-matched IgG were negative controls for primary antibodies.

CYLD expression level was determined by using ImageJ software (National Institutes of Health, Bethesda, MD, USA). (see Supplementary material, Supplementary Materials and Methods for details of scoring)

Cells and cell culture

The human OSCC cell lines SAS and HSC3 were donated by the Cell Resource Center for Biomedical Research, Tohoku University (Sendai, Japan). Non-malignant human HaCaT keratinocytes were kindly provided by Dr P. Boukamp, DKFZ, Heidelberg, Germany. SAS cells were grown in RPMI 1640 medium (Thermo Fisher Scientific, Inc., Waltham, MA, USA) and HSC3 and HaCaT cells were grown in DMEM (Thermo Fisher Scientific, Inc.), supplemented with 10% heat-inactivated FBS (Thermo Fisher Scientific, Inc.), in 5% CO_2 at 37 °C. All cells were authenticated via short tandem repeat fingerprinting by the Japanese Collection of Research Bioresources Cell Bank.

Transfection with siRNA

Cells were transfected with CYLD-specific siRNA (siCYLD) by using Lipofectamine 2000 (Thermo Fisher Scientific, Inc.) according to the manufacturer's protocol. Silencer Negative Control siRNA (Thermo Fisher Scientific, Inc.) was used as the control (siCtrl). Sequences of siCYLD were sense 5′-GAUUGUUACUUCUAUCAAAtt-3′ and antisense 5′-UUUGAUAGAAGUAACAAUCtt-3′. Sequences of siCYLD-UTR, which targets the sequence containing the 3′-UTR lesion of the *CYLD* gene, were sense 5′-GCAGAGUCCUAACGUUGCAtt-3′ and antisense 5′-UGCAACGUUAGGACUCUGCtt-3′ (Thermo Fisher Scientific, Inc.).

RNA isolation and RT-qPCR

Total RNA was isolated from tissue specimens and cultured cells by using the RNeasy Mini Kit (Qiagen, Valencia, CA). Total RNA (0.5 μg) was reverse transcribed to cDNA via the PrimeScript RT reagent (Takara Bio Inc., Shiga, Japan), according to the manufacturer's instructions. Each PCR assay was performed using 2 μl of cDNA and each primer at 0.2 μM in a LightCycler System with SYBR Premix DimerEraser (Takara Bio Inc.). The primers were purchased from Sigma (St Louis, MO, USA). 18S rRNA was used as the internal control. Each reaction (with 20 μl samples) was performed under the following conditions: initialization for 10 s at 95 °C, then 45 cycles of amplification, with 5 s at 95 °C for denaturation and 20 s at 60 °C for annealing and elongation. All standards and samples were analysed in triplicate.

Gene expression microarray

Gel electrophoresis was used to check the integrity of RNA isolated from the cells; two bands, 18S and 28S, indicated satisfactory RNA quality. Affymetrix GeneChip Human Genome U133 Plus 2.0 Array (Affymetrix, Santa Clara, CA, USA) was used for microarray experiments according to the manufacturer's protocol. Hybridization and scanning were done according to the standard Affymetrix procedure. Probe signals were scanned and calculated with a Gene Array scanner (GCS3000 system; Affymetrix). Signals with at least 2.0-fold higher or lower expression were said to represent upregulation and downregulation in CYLD-knockdown SAS cells, respectively. A heat map of selected genes was produced by using Cluster 3.0 and Java

TreeView 1.0.12. Gene expression data sets are available through the Gene Expression Omnibus (GEO) (accession number GSE100589).

To identify significant gene sets enriched by CYLD knockdown in SAS cells, Gene set enrichment analysis (GSEA) was performed using C2 curated functional gene sets from the Molecular Signatures Database (MsigDB) (http://software.broadinstitute.org/gsea/index.jsp). Significant gene sets enriched by CYLD knockdown in SAS cells were identified using a nominal p value < 0.05 and a false discovery rate (FDR) q value < 0.25.

Protein extraction and immunoblotting

Detailed procedures are described in Supplementary material, Supplementary Materials and Methods. Immunoblotting was performed as described previously [26].

Migration assay and invasion assay

Detailed procedures are described in Supplementary material, Supplementary Materials and Methods. We used a wound-healing assay to investigate cell migration. Cell invasive property was assessed by using the CytoSelect 24-Well Cell Invasion Assay Kit (Cell Biolabs, Inc., San Diego, CA, USA).

Luciferase assay

The plasmid for luciferase reporter driven by 4 copies of Smad binding elements (SBE4-Luc) and

Renilla luciferase control reporter vector (pRL-SV40P) were gifts from Ron Prywes (Addgene plasmid # 27163) and Bert Vogelstein (Addgene plasmid # 16495), respectively. SAS cell lines were transfected with siRNA and SBE4-Luc using Lipofectamine 2000 (Thermo Fisher Scientific, Inc.). pRL-SV40P was cotransfected in the cells to normalize for transfection efficiency. At 48 h after transfection, cells were starved for 24 h. Cells were lysed and luciferase activity was determined by using a Dual-luciferase reporter assay system (Promega), according to the manufacturer's manual. The relative luciferase activity was calculated by normalizing firefly luciferase activity to that of Renilla luciferase. Experiments were repeated three times, and relative activity was expressed as mean ± SE.

Statistical analysis

Statistical significance was defined as $p < 0.05$ for Student's *t*-test and χ^2 test. Student's *t*-test was used to compare means of two groups in the *in vitro* experiments. JMP software Version 13 for Windows (SAS Institute Inc., Cary, NC, USA) was used for statistical analysis.

Results

CYLD protein expression is reduced in invasive OSCC lesions

To investigate the role of CYLD in OSCC, we first examined alterations in the *CYLD* gene by analysing the cBioPortal for Cancer Genomics [27,28] and the Catalog of Somatic Mutations in Cancer (COSMIC) database [29,30]. The analyses showed the presence of non-synonymous mutations and copy number alterations in the *CYLD* gene in 2.8% (8/543) and 0.85% (3/353) of head and neck SCC cases, respectively (Supplementary material, Table S1 and S2), with only 1 mutation among 21 upper aerodigestive tract SCC cell lines occurring (Supplementary material, Table S3). These data indicated that gene alterations in *CYLD* gene in OSCC were rare.

Thus, we next performed immunohistochemical analysis with anti-CYLD antibody for oral CIS (n = 45), invasive OSCC (n = 82), and normal oral mucosal tissues (n = 10) to evaluate CYLD expression in OSCC. Laminin γ2 was used as a marker of intact basement membrane [31]. In normal mucosa, CYLD immunoreactivity appeared on basal cells (Figure 1A, left panel); continuous laminin γ2 expression occurred along the basement membrane as expected (Figure 1A, right panel). In CIS OSCC tissues in which laminin γ2-positive basement membrane seemed intact (Figure 1B, right panel), CYLD expression was apparent in 44 (97.8%) out of 45 cases (Figure 1B, left panel). Even tissues obtained from patients with invasive OSCC manifested abundant CYLD expression in cancer cells and atypical cells in a lesion with an intact basement membrane (confirmed by a laminin γ2-positive layer) (Figure 1C, arrowheads in

upper right panel and asterisks). CYLD dominantly localized in cytoplasm of cancer cells as demonstrated in several previous reports [32,33]. In striking contrast, CYLD staining intensity in cancer cells in the invasive lesion was drastically decreased compared with that in the non-invasive lesion (Figure 1C, arrows and daggers in left panels, and 1D). Laminin γ2 is also one of the best-known markers of tumour cells at the invasion front or in budding tumour cells in several types of carcinoma including OSCC [34,35]. Indeed, in the invasive lesion with reduced CYLD expression, tumour cells strongly expressed laminin γ2. In approximately half of cases, cancer cells at an invasive lesion were negative for CYLD (Figure 1E and Supplementary material, Figure S1A). These observations suggest that reduced CYLD expression may be involved in invasion, rather than tumour initiation, in OSCC.

Downregulation of CYLD expression leads to EMT-like changes

To clarify the biological significance of reduced CYLD expression in invasive OSCC, we used siRNA to suppress CYLD expression in OSCC cells and non-malignant HaCaT keratinocytes. Dedifferentiation via EMT previously strongly enhanced cancer cell motility and dissemination [3]. The EMT process is typically accompanied by morphological alterations and expression of fibroblast phenotypic markers, concomitant with downregulation of the epithelial phenotypic marker. Here, CYLD knockdown in the OSCC cell lines, SAS and HSC3, and in HaCaT cells led to a reduction in cell-to-cell contact and elongated spindle-shaped morphology that is representative of mesenchymal cells (Figure 2A). In addition, loss of CYLD increased

expression of mesenchymal markers including fibronectin, N-cadherin and vimentin, plus laminin γ2, a marker of invading cancer cells (Figure 2B and 2C). Basement membrane destruction and extracellular matrix degradation are essential for tumour cell invasion and are usually achieved by proteolytic MMPs [36]. We also found that CYLD downregulation drastically increased expression and activity of MMP9 and/or MMP2, as assessed by RT-qPCR (Figure 2B) and zymography (Figure 2C), respectively. Downregulation of E-cadherin, a typical epithelial cell marker, was not apparent or weak after CYLD knockdown (Figure 2B and 2C).

We next investigated the effects of CYLD knockdown on cell migration and invasion. In our wound-healing assay, CYLD knockdown significantly promoted migration of OSCC cells and HaCaT keratinocytes (Figure 2D). Also, CYLD knockdown significantly increased invasiveness as assessed by the Transwell invasion assay (Figure 2E). We then used transcriptome analysis to investigate global gene expression alterations after siCYLD transfection in SAS cells. As Figure 2F shows, our GSEA based on transcriptome data showed that gene sets associated with mesenchymal features, cell migration, and cell invasion were markedly enriched in CYLD knockdown cells compared with controls, supporting the observed phenotypes confirmed by global molecular evidence. These data indicate that CYLD downregulation in OSCC cells promotes migration and invasion via EMT-like changes, results that are consistent with our immunohistochemical findings (Figure 1).

Downregulation of CYLD expression stabilizes ALK5 protein and enhances TGF-β

signalling

To clarify molecular mechanisms underlying the invasiveness induced by CYLD downregulation, we assessed global gene expression after siCYLD transfection. GSEA demonstrated significant upregulation of potential targets of TGF-β with CYLD suppression (Figure 3A). TGF-β ligands signal via two types of transmembrane serine/threonine kinase receptors: TGF-β receptor I (ALK5) and TGF-β receptor II (TGFβRII). After ligand binding, TGFβRII phosphorylates ALK5, which leads to activation of Smad and non-Smad pathways [7]. Smad proteins are key transducers in TGF-β signalling [7-9]. TGF-β induces Smad2/3 phosphorylation, and phosphorylated Smad2/3 forms heterotrimers with Smad4, translocates to the nucleus, and controls gene expression at Smad-binding elements. Consistent with gene expression results, we found increased Smad3 phosphorylation in CYLD knockdown OSCC cell lines and HaCaT keratinocytes (Figure 3B). In addition, the activity of SBE4-Luc reporter, which contains 4 tandem repeats of Smad-binding elements [37] and measures a Smad3/4-specific response, was induced by transfection of different sequences of siRNA targeting CYLD (Figure 3C). Accordingly, CYLD knockdown increased basal mRNA expression of *SERPINE1*, which is an established Smad-targeted gene (Figure 3D). These data indicate that CYLD downregulation promoted TGF-β signalling.

We then elucidated molecular mechanisms underlying promotion of TGF-β signalling by CYLD knockdown. Our analyses showed increased ALK5 protein in OSCC and HaCaT cells transfected with siCYLD compared with siCtrl concomitantly with increased Smad3

phosphorylation (Figure 3B), although we found no changes at the mRNA level (Supplementary material, Figure S2A). To determine whether post-translational mechanisms are involved in increased ALK5 protein expression, we performed a cycloheximide chase assay and found that CYLD knockdown promoted stability of ALK5 protein in SAS cells and HaCaT keratinocytes (Figure 3E). Also, loss of CYLD enhanced TGF-β-induced *SERPINE1* expression (Figure 3F), as well as the extent and time period of TGF-β-induced Smad3 phosphorylation (Figure 3G). These data indicate that CYLD downregulation promoted ALK5 stabilization and hence TGF-β signalling.

EMT-like changes and invasion induced by CYLD downregulation require ALK5 activity

To determine whether increased ALK5 expression and subsequent TGF-β signalling activation are important for the invasiveness induced by CYLD suppression, we investigated the effects of ALK5 inhibition. Treatment with an ALK5 inhibitor reversed the spindle-shaped morphology to a round clustered epithelial organization shape (Figure 4A) and almost completely suppressed expression of fibronectin and MMP9 (Figure 4B and 4C) induced by CYLD knockdown in SAS cells. ALK5 inhibitor thus significantly suppressed CYLD knockdown-induced cell migration (Figure 4C) and invasion (Figure 4D). These data indicate that EMT-like changes, cell migration, and cell invasion induced by CYLD downregulation depended on increased ALK5 activity. Next, we created a gene set of "TGF-β response signature" from 3 independent previous reports [38-40], and this was overlaid with the genes altered (> 2 or < 0.7-fold change)

by CYLD knockdown in SAS cells. The analysis showed the alteration of TGF-β target genes known to be associated with EMT, metastasis or poor prognosis in head and neck SCC (such as PMEPA1, ANGPTL4, SOX4, CD44, NEDD9, FOXP1, etc.) by CYLD knockdown in SAS cells, and ALK5 inhibition counteracted the altered gene expression profile caused by CYLD knockdown (Figure 4E).

NF-κB is constitutively activated in OSCC [41], and loss of CYLD activates NF-κB signalling [12,14]. As expected, we found an enrichment of genes upregulated by NF-κB activation and a reduction in IκBα protein, which is a key negative regulator of NF-κB in OSCC cells transfected with siCYLD (Supplementary material, Figure S3A and S3B), findings that clearly indicated NF-κB activation by CYLD knockdown. Inasmuch as ALK5 inhibition did not affect the IκB-α protein level that was reduced by CYLD downregulation (Supplementary material, Figure S3B), loss of CYLD likely activated NF-κB independently of TGF-β signalling.

Clinical significance of CYLD downregulation in invasive OSCC

We then investigated the clinical significance of reduced CYLD expression in invasive OSCC and the clinical relevance of the *in vitro* findings described above. Consistent with our immunohistochemical results (Figure 1C), lower CYLD expression was significantly associated with the T4 status in the TNM staging system, defined as deep tumour invasion of surrounding tissues such as bone, skin, and other areas of the head and neck (Figure 5A). Significant

correlations between reduced CYLD expression and increased tumour stage were found (Figure 5A). Kaplan-Meier survival analysis revealed that lower CYLD expression was significantly associated with reduced overall survival in patients with invasive OSCC (log-rank test, $p < 0.05$, Figure 5B). As an important result, our immunohistochemical analyses showed that CYLD expression was inversely correlated with Smad3 phosphorylation ($p < 0.05$, Figure 5C, D), which indicates the clinical relevance of our *in vitro* findings. Taken together, our data thus suggest that decreased CYLD expression, as observed in invasive lesions in OSCC tissues, promotes cell invasion by activating TGF-β signalling through ALK5 stabilization in these cells (Figure 6A).

Discussion

Tumour invasion is the first step in metastasis, which is the leading cause of mortality of patients with cancer including OSCC. Therefore, understanding the mechanisms underlying tumour cell invasion may lead to limiting tumour progression and thus to reduced mortality of OSCC patients. We demonstrated here that cell invasion is promoted by decreased CYLD expression in OSCC cells through EMT-like changes via ALK5 stabilization.

In the present study, our immunohistochemical analyses of OSCC, including CIS and invasive tumours, and normal oral mucosal tissues showed reduced CYLD expression in OSCC cells at invasive lesions. Furthermore, lower CYLD expression was correlated with deep tumour invasion and, consistent with a previous report [42], poor prognosis in patients with invasive OSCC. A recent study showed that defects in CYLD by genetic alterations were accompanied with the maintenance of episomal HPV in head and neck SCC [43] even though genetic alterations in the *CYLD* gene are rare (Supplementary material, Table S1-S3), which suggests the necessity to further investigate the correlation between HPV status and CYLD expression level in OSCC. Our current findings derived from database and immunohistochemical analyses suggest that CYLD downregulation is predominantly associated with tumour progression, including CIS-invasive tumour conversion, rather than tumour initiation in OSCC and that it is likely due to transcriptional and/or post-transcriptional dysregulation. In fact, our *in vitro* studies showed that CYLD knockdown strongly promoted migration and invasion of OSCC cells as well as non-malignant keratinocytes. The invasive behaviour induced by CYLD knockdown was

associated with acquisition of mesenchymal characteristics, as revealed by the altered transcription profile, induction of mesenchymal marker proteins, and increased MMP activity.

Certain studies have shown that TGF-β mediates EMT and proinvasive phenotypes in developmental processes and human cancers, including OSCC [6]. In addition, post-translational regulation of ALK5 has crucial effects on downstream signal transduction, which indicates how this signalling system can produce exquisitely regulated, intricate responses [44]. In the current study, we found that loss of CYLD stabilized ALK5 protein so as to promote TGF-β signalling in OSCC cells, as well as in non-malignant keratinocytes, which led to induction of invasive phenotypes. A recent study of innate immune responses showed that loss of CYLD resulted in Smad3 protein stabilization via increased Akt ubiquitination in tracheal epithelial cells [45], which not only supports our observation that CYLD regulates TGF-β signalling but also suggests the existence of context-dependent mechanisms because stabilization of ALK5 protein was predominant in our study. Smad7 mediates ubiquitination and degradation of ALK5 and Smad2/3 by Smad ubiquitination regulatory factor 2 (Smurf2) [45]. CYLD reportedly formed a complex with Smad7 in response to TGF-β signalling to remove K63-linked polyubiquitin chains on Smad7, which regulates the activity of TGF-β-activated kinase 1 in T cells [46]. This process may also affect the stability of ALK5 or Smad2/3, although this report did not suggest this effect. Notably, we found that treatment of cells with a sufficient amount of anti-TGF-β antibody (clone 1D11; R&D systems, Minneapolis, MN, USA) to suppress TGF-β ligand binding, could not inhibit cell migration induced by CYLD knockdown

(Supplementary material, Figure S4). This preliminary data suggests that, in addition to the increased ALK5 protein level by stabilization, TGF-β ligand-independent ALK5 activation might be involved in the activation of its downstream signalling pathways and induction of migratory phenotype by CYLD knockdown.

Also, loss of CYLD activates NF-κB signalling [12,14]. Our data (Supplementary material, Figure S3A and S3B) indicated that loss of CYLD activated NF-κB independently of TGF-β signalling. However, several NF-κB components have affected ALK5 protein stability or function. TNF receptor-associated factor 4 (TRAF4) reportedly antagonized Smurf2, which led to increased ALK5 stability [47]. In addition, TRAF6, a target of CYLD for deubiquitination [12], ubiquitinates ALK5 and thereby promotes its cleavage and nuclear translocation, which activates genes involved in tumour cell invasiveness [48]. Furthermore, a drug-screening study identified the proton pump inhibitor lansoprazole as a drug that activates TGF-β superfamily bone morphogenetic protein signalling by directly targeting CYLD to block its deubiquitinating activity, which leads to enhanced TRAF6 polyubiquitination, although the receptor level was unknown [49]. Additional investigations of molecular mechanisms underlying CYLD regulation of ALK5 stability may give novel insights into crosstalk between TGF-β signalling and NF-κB signalling or inflammatory responses, with crosstalk having seen increasing interest [50-52].

TGF-β signalling activation in cancer cells contributes to tumour progression in various ways by affecting both tumour cell properties and surrounding microenvironments [53]. Indeed, we found alterations in numerous genes associated with malignant progression, even with our

focus on only TGF-β signalling targets (Figures 2B and 4E). TGFβRII expression was reduced in >70% of head and neck SCCs [54] because of genetic alterations or epigenetic silencing [55]; altered ALK5 expression has been controversial. However, use of oncogenic manipulations causes such TGF-β-non-responsive cells to become more aggressive and metastatic than their responsive counterparts in OSCC and other cancers [53,54]. We found that, possibly because of the increase in ALK5, responsiveness to exogenous TGF-β was markedly enhanced in CYLD-knockdown OSCC cells. One interesting possibility is that OSCC cells at the invasive front with reduced CYLD expression may not only promote invasion but also affect various biological aspects associated with tumour progression including cell proliferation, angiogenesis, drug resistance, and tumour recurrence [53,54], via enhanced TGF-β-responsiveness [56].

Little information is available about molecular mechanisms of CYLD downregulation. Our data suggest that a reduction in CYLD expression triggers CIS-invasive tumour conversion, and thus signal cascades that induce tumour cell invasion at early stages may be responsible for CYLD downregulation in OSCC cells. In this regard, the transcription factor Snail, which is a typical EMT transducer, directly suppressed transcription of the *CYLD* gene to promote migration and invasion of malignant melanoma cells [57]. Also, we previously reported that hypoxia, which promoted tumour cell invasion [58], dramatically suppressed CYLD mRNA expression in glioblastoma cells and OSCC cells [26] (data not shown). Additional studies are needed to clarify the molecular mechanisms underlying CYLD downregulation.

In conclusion, we demonstrated here that downregulation of CYLD enhances TGF-β

signalling via stabilized ALK5 protein in OSCC cells, which promotes tumour cell invasion through EMT-like changes. Our current findings emphasize the importance of using TGF-β signalling inhibitors such as ALK5 inhibitor to block OSCC cell invasion. Additional studies of CYLD regulation of TGF-β signalling may contribute to greater understanding of molecular mechanisms by which tumour cells disseminate and may result in the development of novel therapies for OSCC.

Acknowledgements

The authors thank Aya Higashi, Akiko Hamada, Hiroko Katsura, and Yuka Okumura for technical assistance. The authors' work was supported by Grants-in-Aid for Scientific Research (A) 24249036 (Y. Ando) and (C) 15K09478 (H. Matsui) and 16K11726 (S. Shinriki), and by a Grant-in-Aid for Young Scientists (A) 26713006 (H. Jono) from the Ministry of Education, Culture, Sports, Science and Technology of Japan; by a Grant for Scientific Research by The Sagawa Foundation for Promotion of Cancer Research; by the Kurozumi Medical Foundation; and by the Takeda Science Foundation. No potential conflicts exist.

Author contributions statement

SS, HJ, and HM conceived and carried out the experiments and analysed data. MM, TN, JG, JL, MU, RY, MS, and HN carried out the experiments. YA conceived the experiments. All authors were involved in writing the paper and had final approval of the submitted and published versions.

References

1. Warnakulasuriya S. Global epidemiology of oral and oropharyngeal cancer. *Oral Oncol* 2009; **45:** 309–316.
2. Jimenez L, Jayakar SK, Ow TJ, *et al*. Mechanisms of invasion in head and neck cancer. *Arch Pathol Lab Med* 2015; **139:** 1334–1348.
3. Chaffer CL, San Juan BP, Lim E, *et al*. EMT, cell plasticity and metastasis. *Cancer Metastasis Rev* 2016; **35:** 645–654.
4. Lamouille S, Xu J, Derynck R. Molecular mechanisms of epithelial-mesenchymal transition. *Nat Rev Mol Cell Biol* 2014; **15:** 178–196.
5. Ahmed S, Nawshad A. Complexity in interpretation of embryonic epithelial-mesenchymal transition in response to transforming growth factor-β signaling. *Cells Tissues Organs* 2007; **185:** 131–145.
6. Xu J, Lamouille S, Derynck R. TGF-β-induced epithelial to mesenchymal transition. *Cell Res* 2009; **19:** 156–172.
7. Ikushima H, Miyazono K. TGFβ signalling: a complex web in cancer progression. Nat Rev Cancer 2010; **10**; 415–424.
8. White RA, Malkoski SP, Wang XJ. TGFβ signaling in head and neck squamous cell carcinoma. *Oncogene* 2010; **29:** 5437–5446.

9. Itoh S, ten Dijke P. Negative regulation of TGFβ receptor/Smad signal transduction. *Curr Opin Cell Biol* 2007; **19:** 176–184.

10. Massagué J. TGFβ signalling in context. *Nat Rev Mol Cell Biol* 2012; **13:** 616–630.

11. Bignell GR, Warren W, Seal S, *et al*. Identification of the familial cylindromatosis tumour-suppressor gene. *Nat Genet* 2000; **25:** 160-165.

12. Massoumi R. Ubiquitin chain cleavage: CYLD at work. *Trends Biochem Sci* 2010; **35:** 392–399.

13. Komander D, Lord CJ, Scheel H, *et al*. The structure of the CYLD USP domain explains its specificity for Lys63-linked polyubiquitin and reveals a B box module. *Mol Cell* 2008; **29:** 451–464.

14. Lork M, Verhelst K, Beyaert R. CYLD, A20 and OTULIN deubiquitinases in NF-κB signaling and cell death: so similar, yet so different. *Cell Death Differ* 2017; **24:** 1172–1183.

15. Jono H, Lim JH, Chen LF, *et al*. NF-κB is essential for induction of CYLD, the negative regulator of NF-κB: evidence for a novel inducible autoregulatory feedback pathway. *J Biol Chem* 2004; **279:** 36171–36174.

16. Tauriello DV, Haegebarth A, Kuper I, *et al*. Loss of the tumor suppressor CYLD enhances Wnt/β-catenin signaling through K63-linked ubiquitination of Dvl. *Mol Cell* 2010; **37:** 607–619.

17. Reiley W, Zhang M, Sun SC. Negative regulation of JNK signaling by the tumor suppressor CYLD. *J Biol Chem* 2004; **279:** 55161–55167.

18. Tesio M, Tang Y, Müdder K, *et al*. Hematopoietic stem cell quiescence and function are controlled by the CYLD-TRAF2-p38MAPK pathway. *J Exp Med* 2015; **212:** 525–538.

19. Chen Y, Wang Z, Wang P, *et al*. CYLD negatively regulates Hippo signaling by limiting Hpo phosphorylation in Drosophila. *Biochem Biophys Res Commun* 2014; **452:** 808–812.

20. Rajan N, Elliott RJ, Smith A, *et al*. The cylindromatosis gene product, CYLD, interacts with MIB2 to regulate notch signalling. *Oncotarget* 2014; **5:** 12126–12140.

21. Yang Y, Zhou J. CYLD—a deubiquitylase that acts to fine-tune microtubule properties and functions. *J Cell Sci* 2016; 129**:** 2289–2295.

22. Sun SC. CYLD: a tumor suppressor deubiquitinase regulating NF-κB activation and diverse biological processes. *Cell Death Differ* 2010; **17:** 25–34.

23. Massoumi R, Chmielarska K, Hennecke K, *et al*.
Cyld inhibits tumor cell proliferation by blocking Bcl-3-dependent NF-κB signaling. *Cell* 2006; **125:** 665–677.

24. Nikolaou K, Tsagaratou A, Eftychi C, *et al*. Inactivation of the deubiquitinase CYLD in hepatocytes causes apoptosis, inflammation, fibrosis, and cancer. *Cancer Cell* 2012; **21:** 738–750.

25. Gellibert F, Woolven J, Fouchet MH, *et al*. Identification of 1,5-Naphthyridine Derivatives as a Novel Series of Potent and Selective TGF-β Type I Receptor Inhibitors. *J Med Chem* 2004; **47:** 4494–4506.

26. Guo J, Shinriki S, Su Y, *et al*. Hypoxia suppresses cylindromatosis (CYLD) expression to promote inflammation in glioblastoma: possible link to acquired resistance to anti-VEGF therapy. *Oncotarget* 2014; **5:** 6353–6364.

27. Gao J, Aksoy BA, Dogrusoz U, *et al*. Integrative analysis of complex cancer genomics and clinical profiles using the cBioPortal. *Sci Signal* 2013; **6:** pl1.

28. Cerami E, Gao J, Dogrusoz U, *et al*. The cBio Cancer Genomics Portal: an open platform for exploring multidimensional cancer genomics data. *Cancer Discov* 2012; **2:** 401–404.

29. Forbes SA, Tang G, Bindal N, *et al*. COSMIC (the Catalogue of Somatic Mutations in Cancer): a resource to investigate acquired mutations in human cancer. *Nucleic Acids Res* 2010; **38:** D652–657.

30. Alexandrov LB, Nik-Zainal S, Wedge DC, *et al*. Signatures of mutational processes in human cancer. *Nature* 2013; **500:** 415–421.

31. Mizushima H, Koshikawa N, Moriyama K, *et al*. Wide distribution of laminin-5 gamma 2 chain in basement membranes of various human tissues. *Horm Res* 1998; **50 Suppl 2:** 7–14.

32. Wickström SA, Masoumi KC, Khochbin S, Fässler R, Massoumi R. CYLD negatively regulates cell-cycle progression by inactivating HDAC6 and increasing the level of acetylated

tubulin. *EMBO J* 2010; **29:** 131–144.

33. Massoumi R, Chmielarska K, Hennecke K, Pfeifer A, Fässler R. Cyld inhibits tumor cell proliferation by blocking Bcl-3-dependent NF-kappaB signaling. *Cell* 2006; **125:** 665–677.

34. Patel V, Aldridge K, Ensley JF, *et al*. Laminin-γ2 overexpression in head-and-neck squamous cell carcinoma. *Int J Cancer* 2002; **99:** 583–588.

35. Ono Y, Nakanishi Y, Ino Y, *et al*. Clinicopathologic significance of laminin-5 γ2 chain expression in squamous cell carcinoma of the tongue: immunohistochemical analysis of 67 lesions. *Cancer* 1999; **85:** 2315–2321.

36. Stamenkovic I. Matrix metalloproteinases in tumor invasion and metastasis. *Semin Cancer Biol* 2000; **10:** 415–433.

37. Zawel L, Dai JL, Buckhaults P, *et al*. Human Smad3 and Smad4 are sequence-specific transcription activators. *Mol Cell* 1998; **1:** 611–617.

38. Sargent JL, Milano A, Bhattacharyya S, *et al*. A TGFβ-responsive gene signature is associated with a subset of diffuse scleroderma with increased disease severity. *J Invest Dermatol* 2010; **130:** 694–705.

39. Padua D, Zhang XH, Wang Q, *et al*. TGFβ primes breast tumors for lung metastasis seeding through angiopoietin-like 4. *Cell* 2008; **133:** 66–77.

40. Zavadil J, Bitzer M, Liang D, *et al*. Genetic programs of epithelial cell plasticity directed by transforming growth factor-β. *Proc Natl Acad Sci U S A* 2001; **98:** 6686–6691.

41. Perkins ND. The diverse and complex roles of NF-κB subunits in cancer. *Nat Rev Cancer* 2012; **12:** 121–132.

42. Ge WL, Xu JF, Hu J. Regulation of oral squamous cell carcinoma proliferation through crosstalk between SMAD7 and CYLD. *Cell Physiol Biochem* 2016; **38:** 1209–1217.

43. Hajek M, Sewell A, Kaech S, Burtness B, Yarbrough WG, Issaeva N. TRAF3/CYLD mutations identify a distinct subset of human papillomavirus-associated head and neck squamous cell carcinoma. *Cancer* 2017; **123:** 1778-1790.

44. Xu P, Liu J, Derynck R. Post-translational regulation of TGF-β receptor and Smad signaling. *FEBS Lett* 2012; **586:** 1871–1884.

45. Lim JH, Jono H, Komatsu K, *et al*. CYLD negatively regulates transforming growth factor-β-signalling via deubiquitinating Akt. *Nat Commun* 2012; **3:** 771.

46. Zhao Y, Thornton AM, Kinney MC, *et al*. The deubiquitinase CYLD targets Smad7 protein to regulate transforming growth factor β (TGF-β) signaling and the development of regulatory T cells. *J Biol Chem* 2011; **286:** 40520–40530.

47. Zhang L, Zhou F, García de Vinuesa A, *et al*. TRAF4 promotes TGF-β receptor signaling and drives breast cancer metastasis. *Mol Cell* 2013; **51:** 559–572.

48. Mu Y, Sundar R, Thakur N, *et al*. TRAF6 ubiquitinates TGFβ type I receptor to promote its cleavage and nuclear translocation in cancer. *Nat Commun* 2011; **2:** 330.

49. Mishima K, Kitoh H, Ohkawara B, *et al*. Lansoprazole upregulates polyubiquitination of the TNF receptor-associated factor 6 and facilitates Runx2-mediated osteoblastogenesis. *EBioMedicine* 2015; **2:** 2046–2061.

50. Freudlsperger C, Bian Y, Contag Wise S, *et al*. TGF-β and NF-κB signal pathway cross-talk is mediated through TAK1 and SMAD7 in a subset of head and neck cancers. *Oncogene* 2013; **32:** 1549–1559.

51. Bitzer M, von Gersdorff G, Liang D, *et al*. A mechanism of suppression of TGF-β/SMAD signaling by NF-κB/RelA. *Genes Dev* 2000; **14:** 187–197.

52. Lu T, Tian L, Han Y, *et al*. Dose-dependent cross-talk between the transforming growth factor-β and interleukin-l signaling pathways. *Proc Natl Acad Sci U S A* 2007; **104:** 4365–4370.

53. Pickup M, Novitskiy S, Moses HL. The roles of TGFβ in the tumour microenvironment. *Nat Rev Cancer* 2013; **13:** 788–799.

54. Lu SL, Herrington H, Reh D, *et al*. Loss of transforming growth factor-β type II receptor promotes metastatic head-and-neck squamous cell carcinoma. *Genes Dev* 2006; **20:** 1331–1342.

55. Muro-Cacho CA, Anderson M, Cordero J, *et al*. Expression of transforming growth factor β type II receptors in head and neck squamous cell carcinoma. *Clin Cancer Res* 1999; **5:** 1243–1248.

56. Oshimori N, Oristian D, Fuchs E. TGF-β promotes heterogeneity and drug resistance in squamous cell carcinoma. *Cell* 2015; **160:** 963–976.

57. Massoumi R, Kuphal S, Hellerbrand C, *et al*. Down-regulation of CYLD expression by Snail promotes tumor progression in malignant melanoma. *J Exp Med* 2009; **206:** 221–232.

58. Erler JT, Bennewith KL, Nicolau M, *et al*. Lysyl oxidase is essential for hypoxia-induced metastasis. *Nature* 2006; **440:** 1222–1226.

Figure Legends

Figure 1. CYLD protein expression in OSCC. (A-D) Immunohistochemical analysis with anti-CYLD antibody in normal oral mucosal tissues (A), oral CIS (B), and invasive OSCC (C and D), as compared with laminin γ2 immunoreactivity. Arrowheads and arrows indicate basement membranes and invasive OSCC cells, respectively. (C) The lower left image provides an enlargement of the boxed area in the upper left image. Lower right image is a diagram showing the approximate location of non-invasive and invasive cancer lesion; the asterisks and daggers indicate non-invasive and invasive cancer lesions, respectively. (E) Statistical analysis of CYLD immunoreactivity. ROI was drawn manually covering the invasive cancer lesion and CYLD expression level in each ROI was determined by using ImageJ software. Especially for the cases negative for CYLD staining, invasive front was determined according to the expression pattern of laminin γ2 as assessed by immunohistochemistry in addition to pathological assessment. The graph illustrates the higher the staining intensity score, the lower the percentage of specimens.

Figure 2. Induction of cell migration and invasion by CYLD knockdown via acquisition of mesenchymal features in OSCC cell lines and HaCaT keratinocytes. (A) Cell morphology after transfection with control siRNA (ciCtrl) or siRNA targeting CYLD (siCYLD) in HaCaT, SAS, and HSC3 cells. Scale bar: 100 μm. (B and C) HaCaT, SAS, and HSC3 cells were transfected with siRNA and then incubated for 96 h. Expression of indicated genes and proteins was then evaluated by using qPCR (B) and Western blotting or zymography (MMP9 and MMP2) (C),

respectively. Values are means ± SEM of triplicate samples**.** *$p < 0.05$ vs. siCtrl. The results of Western blotting and zymography are representative of three independent experiments. (D) Cells were wounded at 72 h after siRNA transfection. After incubation for 24 h (HaCaT and HSC3) or 12 h (SAS) in serum-free medium, cell migration was analysed. Migration into the wound area was visualized via phase-contrast microscopy and photographed. Representative photographs of SAS cells appear on the left. Scale bar: 500 μm. The graphs at the right show quantitative results (means ± SEM of triplicate samples). *$p < 0.0005$; †$p < 0.005$. (E) Cells were suspended in serum-free medium with or without ALK5 inhibitor on transwell filters coated with Matrigel in the upper chamber, and medium containing 0.5% serum was used as a chemoattractant in the lower chamber. After 48 h, cells that had invaded were stained. Fluorescence of stained cell-containing solution was read at 480/520 nm. Values are means ± SEM of triplicate samples**.** †$p < 0.005$. (F) GSEA enrichment plots obtained with gene expression data from CYLD knockdown SAS cells (siCYLD) compared with control SAS cells (siCtrl). Normalized enrichment score (NES), nominal *p* values, and FDR *q* values are shown.

Figure 3. Induction of stabilization of ALK5 protein and promotion of TGF-β signalling by CYLD knockdown. (A) GSEA enrichment plot obtained with gene expression data from CYLD knockdown SAS cells (siCYLD) compared with control SAS cells (siCtrl). The PLASARI_TGFB1_TARGETS_10HR_UP plot is representative. NES, nominal *p* value, and FDR *q* value are shown. (B) HaCaT, SAS, and HSC3 cells were transfected with siRNA and

then incubated for 96 h before harvesting. Cell lysate was immunoblotted with antibodies against indicated proteins. (C) SAS cells were transfected with SBE4-Luc, Renilla luciferase control reporter vector, and siRNA. At 48 h after siRNA transfection, cells were starved for 24 h, and then lysed. The relative luciferase activity was calculated by normalizing firefly luciferase activity to that of Renilla luciferase. Experiments were repeated three times, and relative activity was expressed as mean ± SE. $*p < 0.05$. (D) At 48 h after siRNA transfection, cells were starved for 24 h, and then *SERPINE1* mRNA expression was evaluated by using qPCR. $^{\dagger}p < 0.0001$; $^{\S}p < 0.0005$. (E) The cycloheximide (CHX) chase assay was performed 72 h after siRNA transfection, and ALK5 protein expression was analysed via Western blotting. (F) At 48 h after siRNA transfection, cells were starved for 12 h followed by incubation with TGF-β1 (5 ng/ml) for 12 h, and then *SERPINE1* mRNA expression was evaluated by using qPCR. $*p < 0.05$. Values are means ± SEM of triplicate samples**.** (G) At 48 h after siRNA transfection, cells were starved for 12 h followed by incubation with TGF-β1 (5 ng/ml) for the indicated times before harvesting. Smad3 phosphorylation was evaluated by using Western blotting. The results of Western blotting are representative of three independent experiments.

Figure 4. Effects of ALK5 inhibition on invasive phenotypes induced by CYLD downregulation. (A) At 48 h after transfection of different sequences of siRNA targeting CYLD (siCYLD and siCYLD-UTR), SAS cells were treated with ALK5 inhibitor (5 μM) for 24 h in serum-free medium, and cells were then photographed. Scale bars: 200 μm. (B) At 48 h after

siRNA transfection, SAS cells were treated with ALK5 inhibitor (1 μM) for 48 h in serum-free medium, and mRNA expression of fibronectin and MMP9 was then evaluated by using qPCR (left panels) and Western blotting (right panels). Values are means ± SEM of triplicate samples**.** *$p < 0.005$; †$p < 0.0005$; N.S., not significant. The results of Western blotting are representative of three independent experiments. (C) At 48 h after siRNA transfection, cells were treated with the indicated concentrations of ALK5 inhibitor for 48 h in serum-free medium. After cells were wounded, they were incubated for 26 h (HaCaT), 6 h (SAS), or 24 h (HSC3) in serum-free medium, after which cell migration was analysed. Representative photographs of SAS cells are shown (upper panels). Scale bar: 500 μm. Values are means ± SEM of triplicate samples**.** *$p < 0.0005$; †$p < 0.05$; §$p < 0.005$; N.S., not significant. (D) SAS cells transfected with siRNA were plated on Matrigel-coated Transwell filters in the upper chamber in serum-free medium with or without 5 μM ALK5 inhibitor. Medium containing 0.5% serum was used as a chemoattractant in the lower chamber. After 48 h, cells that had invaded were stained. Fluorescence of stained cell-containing solution was read at 480/520 nm. Values are means ± SEM of triplicate samples**.** *$p < 0.0005$; §$p < 0.005$. (E) A heat map of representative TGF-β-target genes in SAS cells treated with DMSO or ALK5 inhibitor after CYLD siRNA transfection. We created a gene set of "TGF-β response signature" from 3 independent previous reports [38-40], and this was overlaid with the genes altered (> 2 or < 0.7-fold change) by CYLD knockdown in SAS cells. Representative "TGF-β target genes" were shown.

Figure 5. Clinical significance of CYLD downregulation in OSCC. (A) Statistical association of CYLD staining score and tumour size (T) and tumour stage (Stage) in OSCC patients. (B) Kaplan-Meier plot of overall survival of OSCC patients with tumours expressing low or high CYLD. (C) Immunohistochemical analysis of CYLD and pSmad3 in invasive OSCC tissues. Scale bar: 200 μm. (D) Percentage of specimens with low or high CYLD expression compared with pSmad3 expression levels. pSmad3 expression level was determined based on the percentage of cells stained at different intensities (see Supplementary material, Supplementary Materials and Methods for details of scoring). $*p < 0.05$ (Pearson's χ^2 test).

Figure 6. A schematic model illustrating the induction of OSCC invasion by CYLD downregulation. (A) Downregulation of CYLD enhances TGF-β signaling, i.e. Smad3 phosphorylation, via stabilized ALK5 protein in OSCC cells, which promotes tumour cell invasion through EMT-like changes.

Supplementary Material Online

Supplementary Materials and Methods **YES**

Supplementary Figure Legends **YES**

Figure S1. Representative picture for each CYLD staining score determined by immunohistochemistry

Figure S2. *ALK5* mRNA expression after CYLD knockdown

Figure S3. NF-κB activation by CYLD knockdown in OSCC cells

Figure S4. Effect of anti-TGF-β antibody on cell migration induced by CYLD knockdown

Table S1. Mutation and CNV in the *CYLD* gene in head and neck SCC

Table S2. List of *CYLD* gene mutations

Table S3. Mutation in the *CYLD* gene in upper aerodigestive tract SCC cell lines

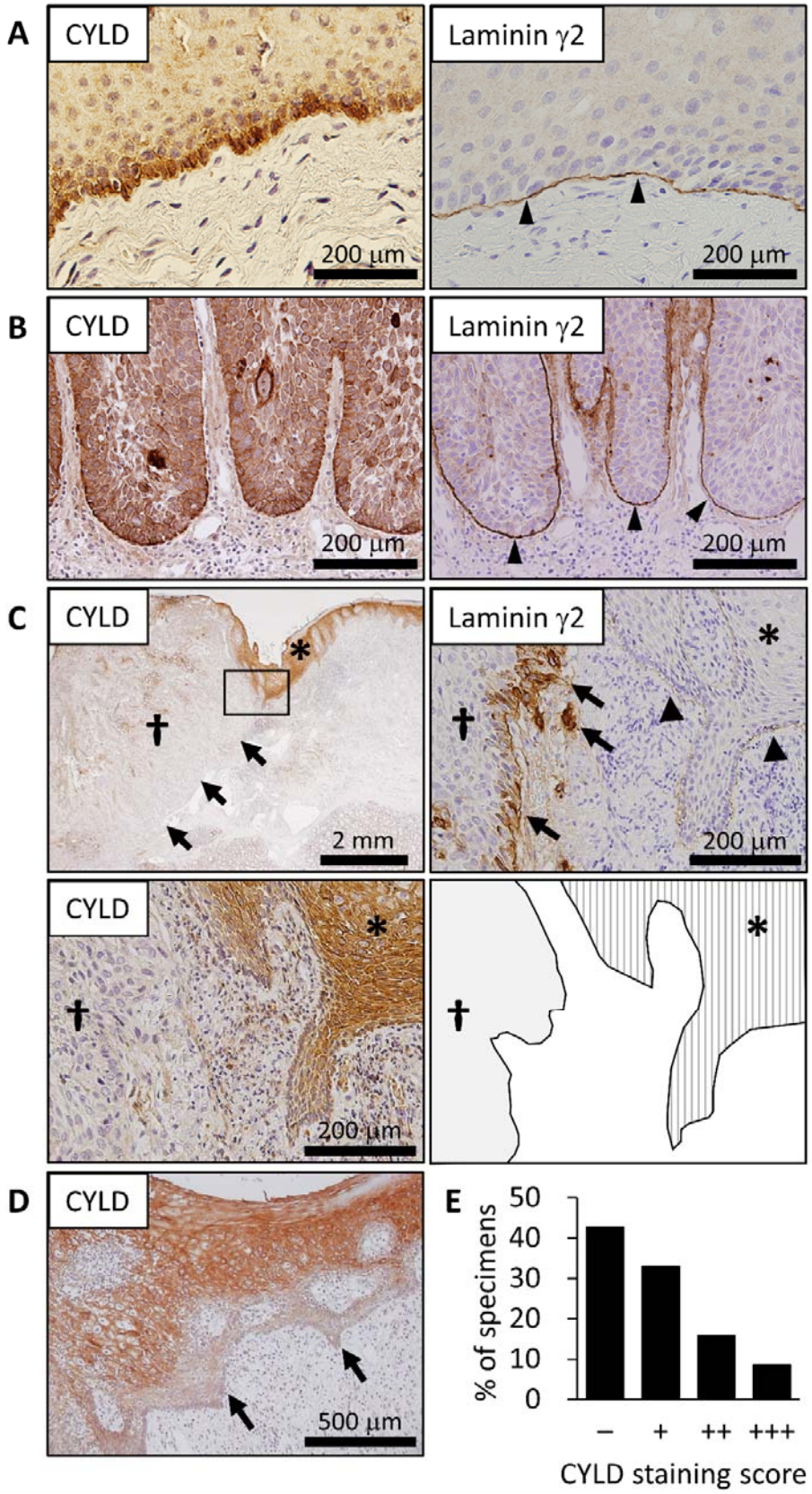

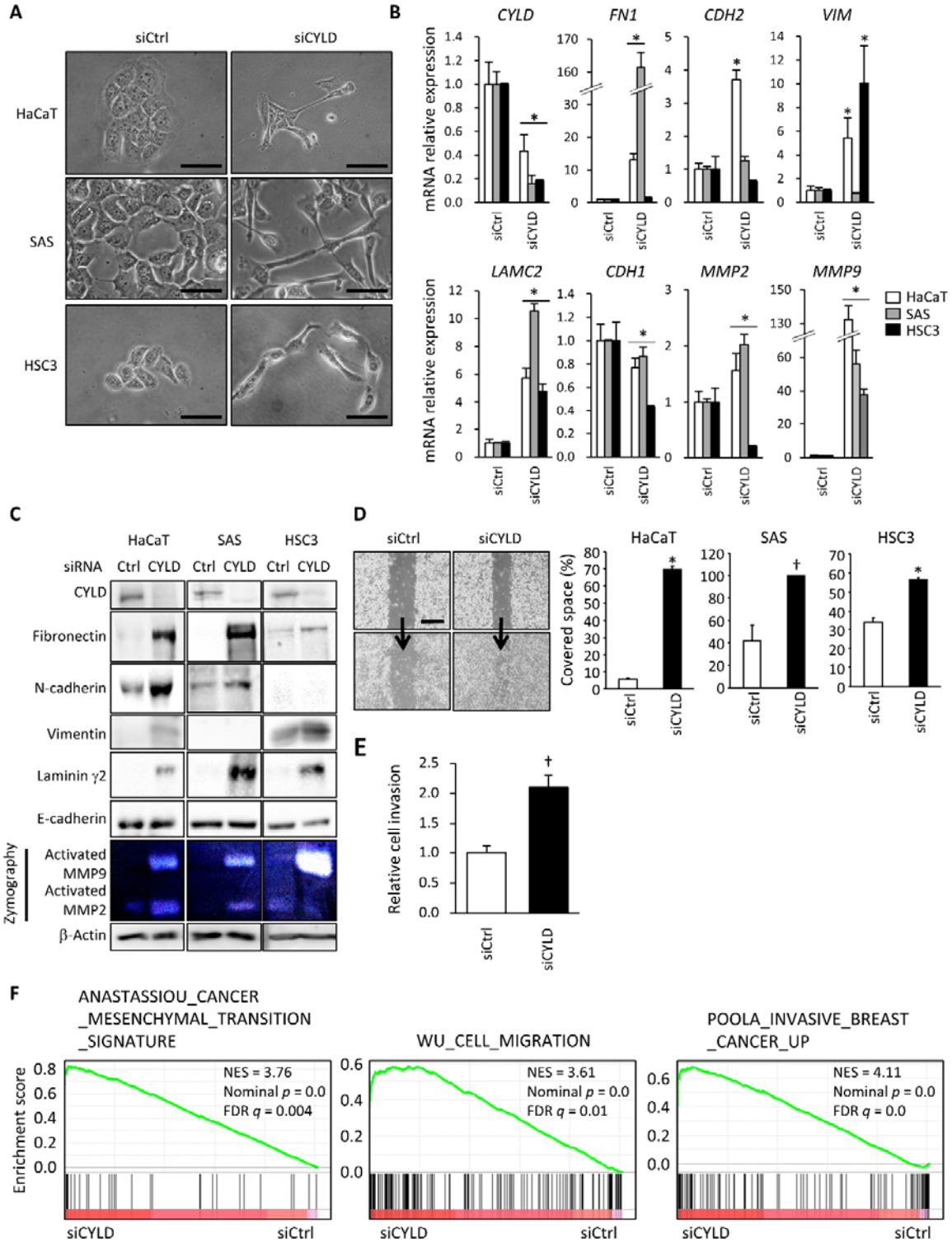

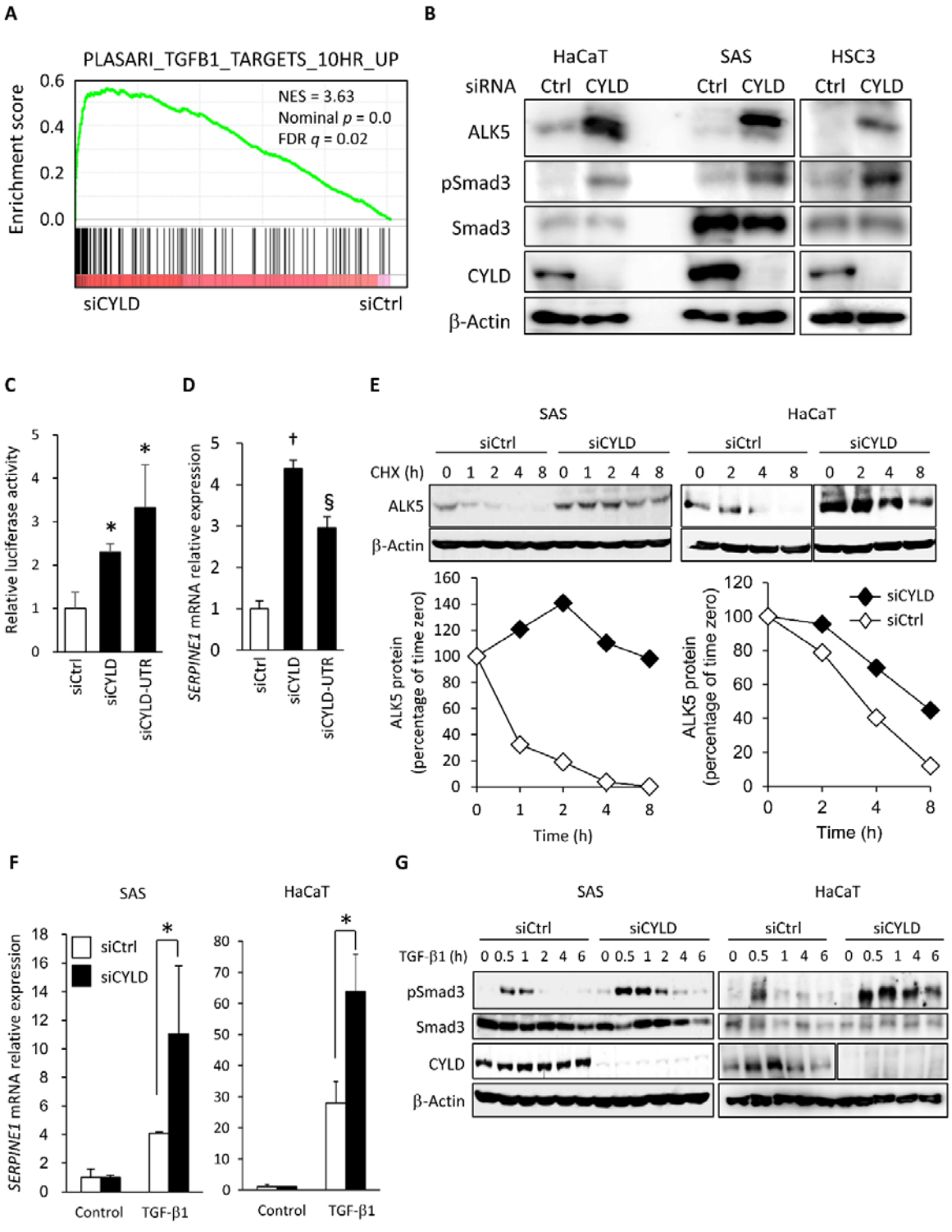

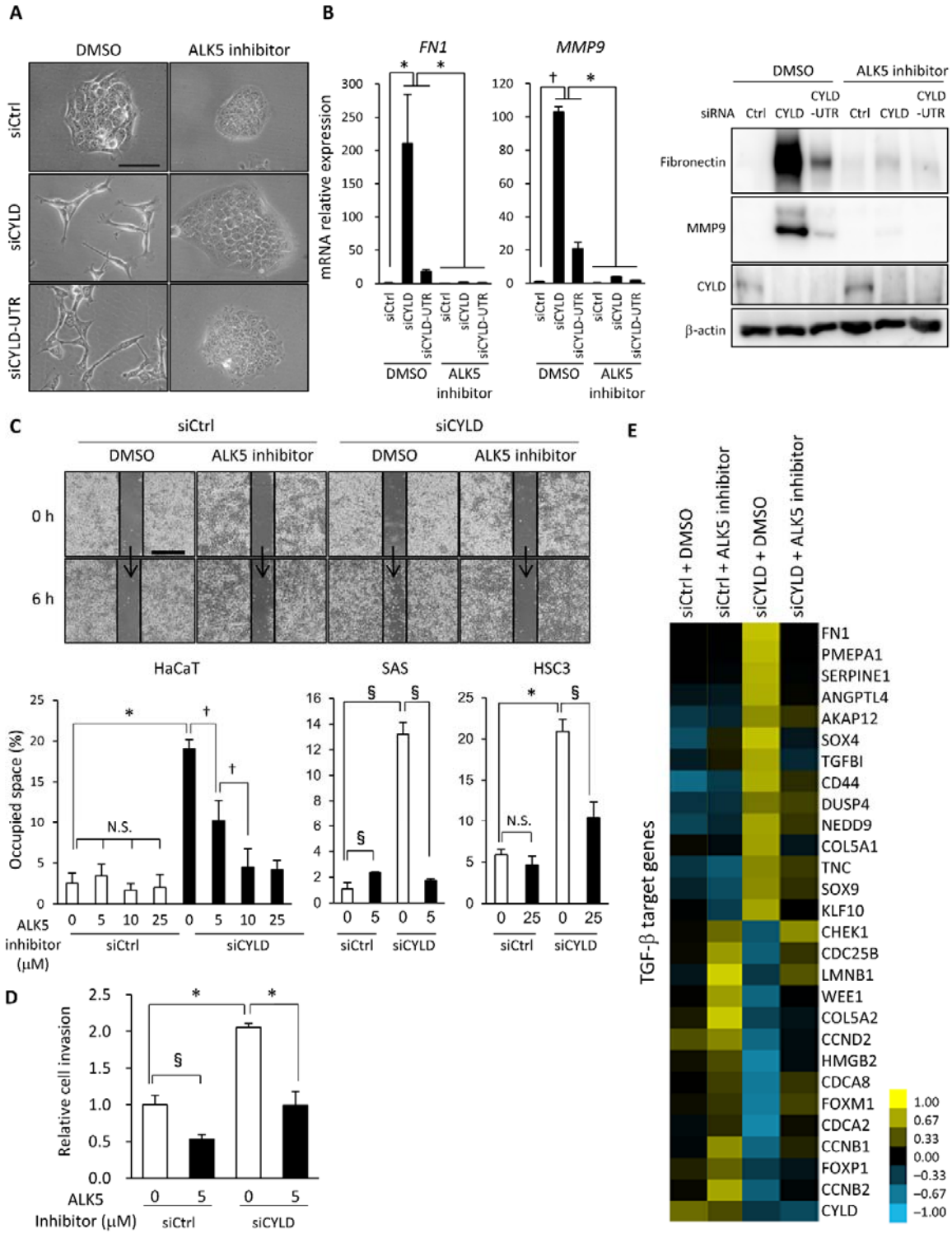

A

Variables	CYLD score Low	High	*p*-value
T			
T1-T3	37	19	0.032
T4	25	1	
Stage			
I-III	20	12	0.027
IV	42	8